Leroy, J. L., Broseta, D., & Guéron, M. (1985b) *J. Mol. Biol. 184*, 165–178.
Loomis, R. E., & Alderfer, J. L. (1986) *Biopolymers 25*, 571–600.
Major, P. P., Egan, E., Herrick, D., & Kufe, D. W. (1982) *Cancer Res. 42*, 3005–3009.
Massoulie, J., Michelson, A. M., & Pochon, F. (1966) *Biochim. Biophys. Acta 114*, 16–26.
Maxam, A. M., & Gilbert, W. (1980) *Methods Enzymol. 65*, 499–560.
Mirau, P. A., & Kearns, D. R. (1984) *J. Mol. Biol. 177*, 207–227.
Mirau, P. A., & Kearns, D. R. (1985) *Biopolymers 24*, 711–724.
Pardi, A., & Tinoco, I. (1982) *Biochemistry 21*, 4686–4693.
Pardi, A., Morden, K. M., Patel, D. J., & Tinoco, I. (1982) *Biochemistry 21*, 6567–6574.
Pardi, A., Morden, K. M., Patel, D. J., & Tinoco, I. (1983) *Biochemistry 22*, 1107–1113.
Patel, D. J. (1974) *Biochemistry 13*, 2396–2402.
Patel, D. J., & Hilbers, C. (1975) *Biochemistry 14*, 2641–2656.
Patel, D. J., Kozlowski, S. A., Marky, L., Broka, C., Rice, J. A., Itakura, K., & Breslauer, K. J. (1982a) *Biochemistry 21*, 428–436.
Patel, D. J., Kozlowski, S. A., Marky, L., Rice, J. A., Broka, C., Dallas, J., Itakura, K., & Breslauer, K. J. (1982b) *Biochemistry 21*, 437–444.
Patel, D. J., Kozlowski, S. A., Marky, L. A., Rice, J. A., Broka, C., Itakura, K., & Breslauer, K. J. (1982c) *Biochemistry 21*, 445–451.
Patel, D. J., Kozlowski, S. A., & Bhatt, R. (1983a) *Cold Spring Harbor Symp. Quant. Biol. 47*, 197–206.
Patel, D. J., Kozlowski, S. A., & Bhatt, R. (1983b) *Proc. Natl. Acad. Sci. U.S.A. 80*, 3908–3912.
Patel, D. J., Kozlowski, S. A., Ikuta, S., & Itakura, K. (1984) *Biochemistry 23*, 3218–3226.
Patel, D. J., Kozlowski, S. A., Weiss, M., & Bhatt, R. (1985) *Biochemistry 24*, 936–944.
Quignard, E., Têoule, R., Guy, A., & Fazakerley, G. V. (1985) *Nucleic Acids Res. 13*, 7829–7836.
Schuetz, J. D., Wallace, H. J., & Diasio, R. B. (1984) *Cancer Res. 44*, 1358–1363.
Szer, W., & Shugar, D. (1963) *Acta Biochem. Pol. 10*, 219–231.
Wempen, I., & Fox, J. J. (1964) *J. Am. Chem. Soc. 86*, 2474–2477.
Wilkinson, D. W., & Crumley, J. (1977) *J. Biol. Chem. 252*; 1051–1056.

Cytochrome *c* Orientation in Electron-Transfer Complexes with Photosynthetic Reaction Centers of *Rhodobacter sphaeroides* and When Bound to the Surface of Negatively Charged Membranes: Characterization by Optical Linear Dichroism†

David M. Tiede
Chemistry Division, Argonne National Laboratory, Argonne, Illinois 60439
Received July 21, 1986; Revised Manuscript Received October 9, 1986

ABSTRACT: Heme orientation with respect to the membrane normal has been measured for the cytochromes *c* and c_2 bound to photosynthetic reaction centers from *Rhodobacter* (*Rhodopseudomonas*) *sphaeroides* R-26 in reconstituted phosphatidylcholine vesicles. Previous kinetic studies have suggested that each cytochrome may bind in two configurations, which lead to either rapid or slow electron transfer to the flash-oxidized reaction center bacteriochlorophyll dimer. The rapid oxidation of cytochrome *c* is ~20-fold slower than that of cytochrome c_2. Optical linear dichroism measurements reported here show that, for both cytochromes, only the population undergoing rapid oxidation is dichroic. A stoichiometry of 0.5 dichroic cytochrome *c* or c_2 is found bound per reaction center. Prominent differences between the dichroism of the cytochrome c_2–reaction center complex and that of the cytochrome *c*–reaction center complex show that heme orientation differs in the two cases. The dichroism of cytochrome *c* bound to the reaction center can be distinguished from its dichroism when bound to the surface of negatively charged membranes. Analysis of the dichroism spectra suggests that, for cytochrome c_2, the heme is tilted 7°–8° closer to the membrane normal and rotated by 32° compared to the cytochrome *c*–reaction center complex. The dichroism spectra are consistent with the notion that the site on the cytochrome *c* surface that binds to the reaction center is the same site that binds to mammalian cytochrome *c* oxidase and reductase. However, a different locus is implicated on the surface of cytochrome c_2. These data suggest that although the tertiary structures of the cytochromes are homologous, the binding site is not conserved. These differences in cytochrome orientations may be in part responsible for the differences in the rate of electron transfer to the reaction center.

The mitochondrial cytochromes *c* and bacterial cytochromes c_2 form a single structural class (Meyer & Kamen, 1982). Cytochromes from both families show a similar conserved protein folding pattern and solvent-exposed heme edge. Yet variations in the specific amino acid sequences produce cytochromes that vary in net charge and redox potential (Bartsch, 1978; Meyer & Kamen, 1982; Meyer et al., 1983). It is expected that these variations optimize electron transfer by

† Supported by fellowships from the NSF–CNRS U.S.–France Exchange of Scientists Program and the Centre Nationale de la Recherche Scientifique and by Department of Energy Contract W-31-109-ENG-38.

0006-2960/87/0426-0397$01.50/0

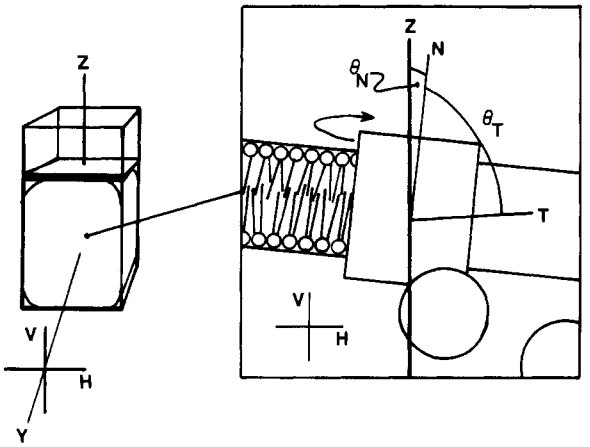

FIGURE 1: Geometry for linear dichroism measurements in squeezed polyacrylamide gels. Gels are placed in a 1-cm cuvette and compressed along the z direction. Optical absorption is measured along an axis perpendicular to this, with linearly polarized light having the electric vector either vertical (V) or horizontal (H). The inset illustrates the mechanical alignment of the reaction center reconstituted membranes, along with bound cytochrome c, induced by the collapse of the polyacrylamide matrix. The membranes tend to orient with the membrane normal (n) aligned along the gel compression direction. The angle θ_n characterizes the extent of membrane alignment for the ensemble of membranes. The angle θ_T is the tilt of an optical transition moment with respect to the membrane normal.

regulating cytochrome binding and orientation in complexes formed with the physiological reaction partners, but little is known of how this is accomplished. The most detailed proposals come from hypothetical interprotein electron-transfer complexes constructed from the individual X-ray structures of cytochrome c and various reaction partners (Salemme, 1976; Poulos & Kraut, 1980; Matthew et al., 1983). Covalent modifications of surface lysine residues have mapped out regions on the cytochrome c surface likely to be involved in "docking" of the cytochrome on its reaction sites (Capaldi et al., 1982; Koppenol & Margoliash, 1982). In this paper optical linear dichroism techniques have been used to quantitate c cytochrome orientations in electron-transfer complexes formed with the photosynthetic reaction center of *Rhodobacter (Rhodopseudomonas) sphaeroides R-26*. This work provides an experimental measure of cytochrome orientation that can be combined with future work on electrostatic and redox parameters to provide a more detailed description of how changes in cytochrome primary structure affect its interprotein electron transfer.

The *R. sphaeroides* reaction center is an integral membrane protein with a molecular weight of approximately 10^5 (Okamura et al., 1982) and a pI of 6.1 (Prince et al., 1974). A light-induced, ~200-ps electron transfer between donor and acceptor molecules (P^+A^-) produces both oxidant and reductant for an energy-conserving electron-transfer chain (Dutton & Prince, 1978; Crofts & Wraight, 1983). The electron donor P is a bacteriochlorophyll dimer (Norris et al., 1974; Lubitz et al., 1984; Mar & Gingras, 1984; Deisenhofer et al., 1984). Cytochrome c_2 ($E_{m,7}$ = 345 mV; pI = 5.5) is the natural donor to the ground-state cation P^+ [$E_{m,7}(P^+/P)$ = 490 mV] (Dutton & Prince, 1978; Crofts & Wraight, 1983), but mitochondrial cytochrome c ($E_{m,7}$ = 245 mV; pI = 10.65) will also substitute for this reaction (Ke et al., 1970; Prince et al., 1974). Kinetic studies have shown that the reaction scheme is the same for both cytochromes (Dutton et al., 1976; Overfield et al., 1979; Overfield & Wraight, 1980a,b; Rosen et al., 1980, 1983).

A dissociation constant, K_d, has been measured to be 1–10 μM for both cytochromes (cyt) (Overfield et al., 1979; Overfield & Wraight, 1980; Rosen et al., 1980). Cross-linking and immunochemical inhibition (Rosen et al., 1983) have shown that cyt c and c_2 bind at the same site on the reaction center. At low salt and high cytochrome concentrations a first-order, cytochrome-independent rate constant (k_f) of (0.3–1) × 10^6 s^{-1} has been measured for cyt c_2, while an ~10-fold slower rate constant of 5 × 10^4 s^{-1} is seen for cyt c (Overfield et al., 1979; Overfield & Wraight, 1980; Rosen et al., 1980). At low cytochrome concentrations, or with high salt, cytochrome oxidation proceeds by a slower, second-order reaction. However, several reports (Dutton et al., 1976; Overfield et al., 1979; Overfield & Wraight, 1980) have found that the second-order reaction reaches a pseudo-first-order limit, where cytochrome oxidation is biphasic, consisting of a fast phase (~50% of total) with k_f as described above and the remainder a slow phase with a rate constant (k_s) of (1.7–3.5) × 10^3 s^{-1}. This has suggested the model where there are two kinds reaction center–cytochrome complexes (Dutton & Prince, 1978; Overfield et al., 1979), which differ in the rate of electron transfer:

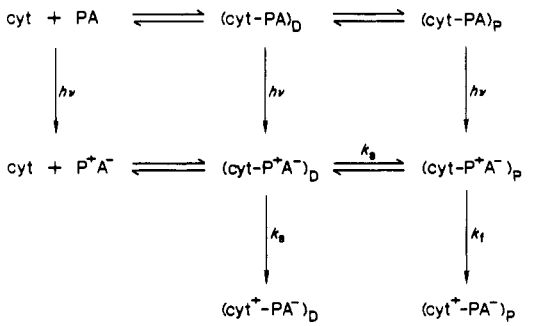

Differences between the two complexes have been attributed to cytochrome bound in favorable "proximal" and unfavorable "distal" configurations for electron transfer (Dutton & Prince, 1978; Moser et al., 1984).

In this paper optical linear dichroism measurements have been used to compare heme orientation in electron-transfer complexes formed between cytochromes c and c_2 and the *R. sphaeroides* reaction center in reconstituted phosphatidylcholine vesicles. Two kinds of dichroism measurements have been made. First, the dichroism of the flash-induced cytochrome c and c_2 absorbance changes has been determined. These measurements determine the dichroism for the population of cytochromes bound at the reaction center oxidation sites and are capable of cistinguishing heme orientation for different kinetic populations. Second, the dichroism of the total cytochrome absorption has also been measured, which provides a measure of the total number of dichroic c cytochrome binding sites. These experiments show that only the cyt c and c_2 populations bound to sites yielding fast oxidation are dichroic. The dichroisms of cyt c and c_2 are different and can be distinguished from their dichroism when bound to the surface of negatively charged lipid membranes. These dichroism measurements suggest possible domains on the cytochrome c and c_2 surface that are responsible for binding to the reaction center and negatively charged membrane.

Materials and Methods

Preparation of Reconstituted Reaction Center Vesicles. Reaction centers from *R. sphaeroides* R-26 were isolated with the detergent lauryldimethylamine oxide (LDAO) according to the procedures described by Wraight (1979). The LDAO was exchanged for sodium cholate by precipitating the reaction

centers with ammonium sulfate, resuspending in 0.5% sodium cholate (w/w)–10 mM tris(hydroxymethyl)aminomethane (Tris) pH 7.8, and dialyzing against 0.5% sodium cholate–10 mM Tris pH 7.8, at 4 °C. Vesicles were prepared by dialysis removal of the cholate in the presence of phosphatidylcholine. To do this, the reaction center concentration was adjusted to 10 μM, the sodium cholate increased to 1%, and phosphatidylcholine from egg yolk (Sigma) added to 1 mM. The solution was dialyzed against 10 mM Tris, pH 7.8, for 48 h at 4 °C, with at least three exchanges of the external solution. Vesicles were pelleted by ultracentrifugation (100000g, 180 min) and resuspended to a reaction center concentration of about 50 μM in 10 mM Tris, pH 7.8, supplemented with 100 μM ubiquinone 10 and sonicated at 4 °C with a probe sonicator (Branson) for 1 min (3 times 20 s) just prior to use. The reaction center concentration was determined by the 802-nm bacteriochlorophyll absorbance, with an extinction coefficient of 288 mM^{-1} cm^{-1} (straley et al., 1973).

Horse heart cytochrome c (type III) was obtained from Sigma and cytochrome c_2 isolated from *R. sphaeroides* R-26 as described by Bartsch (1978). The cytochrome concentration was determined from the reduced absorption spectra, with extinction coefficients of 27.6 and 30.8 mM^{-1} cm^{-1} for cyt c and c_2, respectively (Bartsch, 1978).

Preparation of Negatively Charged Lipid Vesicles. Vesicles with varying ratios of phosphatidylcholine, PC (from egg yolk, Sigma), to phosphatidylinositol, PI (soybean, Sigma), were prepared from chloroform solutions of the lipids, which were dried under nitrogen; 10 mM Tris buffer was then added to the tube to bring the total lipid concentration to 6 mM. Vesicles were formed by four 30-s periods of sonication at 22 °C, separated by 1-min intervals.

Preparation of Oriented Membranes in Squeezed Polyacrylamide Gels. The reaction center reconstituted membrane vesicles or mixed PC + PI vesicles were orientated by incorporation into polyacrylamide gels (Abdourakhmanov et al., 1979; Haworth et al., 1982; Tapie et al., 1982). The gel-forming mixture, with final concentrations of 8.5% acrylamide, 2.5% bis(acrylamide), 0.23% tetramethylethylenediamine (TEMED), 0.05% ammonium persulfate, and 10 mM Tris, pH 7.8, was allowed to react for 2 min in a 0.8-cm internal diameter, stoppered tube before the vesicle suspensions (10% final gel volume) and cytochrome c or c_2 (diluted from 5 mM stocks) were quickly added and mixed. The gels polymerized after ~1 min following vesicle and cytochrome additions. During this time, gels were cooled with running water. The polymerized gels were removed from the tubes and placed in 10 mM Tris, pH 7.8, for 1 h, with 50 μM 1,4-dihydroxynaphthoquinone, which served as an electron acceptor for the reaction center ubiquinone, and 1 mM sodium ascorbate to reduce the cytochrome.

Membrane orientation was induced by placing an ~1.5-cm section of the gel in a standard 1-cm path-length cuvette and compressing the gel to ~70% of the original length. Squeezed polyacrylamide gels have been used extensively to orient detergent-solubilized membrane proteins and chloroplast thylakoids (Abdourakhmanov et al., 1979; Haworth et al., 1982; Tapie et al., 1982; Kramer et al., 1984). The collapse of the acrylamide matrix in the compressed gels mechanically aligns anisotropic particles with their long axis perpendicular to the compression direction. In the case of the membrane samples, the normal to the membrane surface tends to align along the compression direction. For spherical vesicles, it is likely that the osmotic gradient across the vesicle membrane in the gel-forming mixture first causes the vesicle to deflate [e.g., Hotani (1984)], which then allows them to be mechanically aligned by compressing the acrylamide matrix.

The special advantage of using acrylamide gels is that the membranes are oriented in a mainly aqueous environment, as opposed to the more usual dehydration methods used to construct oriented membrane multilayers. Evidence that the incorporation of membrane vesicles into polyacrylamide gels does not appreciably disrupt native membrane structure is suggested by assays of electrical membrane potential formation in bacterial photosynthetic membranes (chromatophores) incorporated in the polyacrylamide gels (Tiede et al., 1984). Kinetics of the formation and decay of the carotenoid absorbance shifts were unaltered from those in aqueous solution. This suggested that the polymerization reaction affected neither the formation nor the decay of the membrane potential. In addition, the flash-induced redox reactions and inhibitor sensitivities of the reaction center and cytochrome b/c_1 components were similarly unaltered (Tiede et al., 1984). Finally, the oxidation kinetics and binding constants found here for the cytochrome c and c_2 with reaction center reconstituted vesicles in acrylamide gels agree with values previously reported in aqueous solution.

Dichroism Measurements. Optical absorption measurements were made at right angles to the squeezing direction with light linearly polarized either parallel to the gel compression axis, A_v, or perpendicular to it, A_H, as indicated in Figure 1. In the case of ideal membrane alignment, this would correspond to absorption parallel or perpendicular to the membrane normal. Linear dichroism spectra ($A_V - A_H$) were recorded with an instrument described previously (Breton, 1974; Tapie et al., 1983). The instrument used a photoelastic modulator to rotate the plane of the polarized light and modulated, lock-in detection. Alternatively, A_V and A_H were recorded separately on a Cary 17 spectrophotometer, using Glan-Thompson prism polarizers.

Dichroism of light-induced absorbance transients was measured on an instrument of local design (Vermeglio et al., 1978). A neodymium YAG pumped rhodamine dye laser (Quantel) provided flash excitation. Single-beam, single-wavelength absorbance transients detected with either a photomultiplier (S-20) or a photodiode were stored in a Tracor-Northern 1500 digitizing signal averager. Data were taken with a time resolution of 10 μs/point. Signal averaging was done by alternating sets of A_V, A_H signal transients, with 30 s between laser flashes to allow for quinone reoxidation and cytochrome rereduction. Absorbance transients were accumulated *after* the initial 10–15 flash excitations. This was done because the extent of cytochrome oxidation diminished during this period and then reached a constant value, independent of flash number. The diminution of the extent of cytochrome oxidation appeared to result from a population of reaction centers (30–50% depending on the preparation) that were progressively inactivated by reduction of the quinone acceptor and were not rapidly reoxidized by the 1,4-naphthoquinone. Throughout the experiment the cytochrome was completely rereduced after each flash, the absorption spectra showed the reaction center bacteriochlorophyll dimer to be fully reduced, and the proportion (<5%) of flash-oxidized reaction centers that were not rapidly reduced by cytochrome was unchanged. Similar behavior was seen for reaction centers in solution, indicating that the slow equilibration of the quinone acceptor in a portion of the reaction centers was not an artifact induced by the acrylamide gels.

Dual-wavelength cytochrome traces (e.g., 550 nm–540 nm) were obtained by subtraction of single-wavelength measurements, following correction of the reference beam for the small wavelength dependence in the contribution of the reaction center to absorbance changes in the 540–580-nm region [e.g., see Rafferty and Clayton (1979)].

Analysis of Dichroism Measurements. The squeezed polyacrylamide gels produce uniaxially oriented samples, in which membranes tend to orient with the membrane normal along the direction of compression. For absorption bands arising from a transition polarized along a single molecular axis, the ratio of the linear dichroism ($A_V - A_H$) and unpolarized absorption A is related to the order parameter S, which describes the extend to which the transition moment is aligned along the orientation axis (Breton & Vermeglio, 1983; Johansson & Lindblom, 1980):

$$\frac{A_V - A_H}{3A} = S = \frac{3\cos^2\theta - 1}{2}$$

θ is the effective angle between the transition moment and the gel orientation axis for the entire ensemble of molecules. The parameter S varies from a value of 1 when θ is 0° to –0.5 when θ is 90°. The measured dichroism can be factored to component S_T, which is the extent of orientation between the transition moment and the membrane normal, and S_M, which is the extent of orientation induced between the membrane normals and the gel orientation axis: $S = S_T S_M$ (Nabedryk & Breton, 1980).

As described under Results, the membrane orientation parameter S_M has been estimated for the reaction center reconstituted vesicles in squeezed gels by comparing the dichroism observed here for the bacteriochlorophyll dimer to the orientation S_T estimated previously for reaction centers in chromatophore membranes (Rafferty & Clayton, 1979). These comparisons indicate that for the membrane-reconstituted reaction centers the degree of orientation obtained between the membrane normal and the gel axis has a range of $0.8 \leq S_M \leq 1$.

Model calculations on the absorption spectrum for chlorophyll (Gouterman, 1961) and a large body of polarized absorption data on the reaction center (Breton & Vermeglio, 1982; Hoff, 1982) suggest that the reaction center bacteriochlorophyll dimer Q_y (860 nm) and Q_x (600 nm) absorptions are each composed of a single π–π^* transition polarized along different molecular directions, forming an angle of 105° (Rafferty & Clayton, 1979; Tiede & Dutton, 1981). For monomeric chlorophyll, the $Q_{x,y}$ transitions lie in the molecular plane, and the angle θ_n between the normal to the molecular plane and the orientation axis can be calculated from a determination of θ for each transition moment and by knowing the angle between them, Φ (Cherry et al., 1972):

$$\sin^2\theta_n = \cos^2\theta_x + \cos^2\theta_y + \cos^2\Phi - 2\cos\Phi\cos\theta_x\cos\theta_y$$

For the more symmetric heme group, the in-plane π–π^* B(0–0) (Soret, 400 nm region) and Q(0–0) (α-band, 550-nm region) transitions are nearly degenerate in the molecular x and y directions (Gouterman, 1978; Adar, 1978; Hofricher & Eaton, 1976). Yet polarized absorption spectra of single ferricytochrome c crystals and ferrocytochrome c in polyvinyl alcohol films (Vermeglio et al., 1980) have shown that the absorptions in the x and y directions are not completely equivalent (Eaton & Hochstrasser, 1976). This is also clearly suggested by low-temperature spectra of ferrocytochrome c and c_2 (Figures 10 and 11), which show the α-band to resolve into two components, A_x and A_y. This suggests that the room temperature α-band absorption and linear dichroism arise from the overlapping A_x and A_y components as well as a component A_b due to the adjacent β-band absorptions:

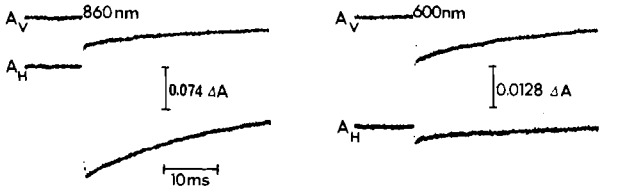

FIGURE 2: Flash-induced absorption changes for reaction center vesicles in squeezed polyacrylamide gels. The 860- and 600-nm absorption changes arise due to the flash oxidation of the reaction center bacteriochlorophyll dimer. On the left are the 860-nm transients, measured with light polarized vertically, ΔA_V (top), or horizontally, ΔA_H (bottom). The corresponding 600-nm traces are shown on the right. The reaction center concentration was 1 μM, and the sample contained 20 μM oxidized cytochrome c.

$$A = A_x + A_y + A_b$$

$$A_V - A_H = D_x A_x + D_y A_y + D_b A_b$$

where $D_i = (A_V - A_H)_i / A_i$ for $i = x$, y, and b. The linear dichroism coefficients D_i are directly related to the order parameter, $D_i = 3S_i$, and may have values between 3 and –1.5. If the dichroisms for A_x and A_y are not identical, the shape of the dichroism spectrum can differ from that of the absorption spectrum.

A nonlinear least-squares fitting program (Minpack-1, Argonne National Laboratory) was used to simultaneously fit both absorption and linear dichroism spectra with these two relations. Fits to the low-temperature absorption spectra were used first to find the integrated absorption intensities for A_x and A_y. Integration of the low-temperature and room temperature absorption spectra showed that the area under the α-band remained constant. The fitting procedure held the areas for A_x and A_y constant and equal to the low-temperature values but allowed the line widths and positions to vary in order to simultaneous fit the room temperature A and $A_V - A_H$ spectra. Lorentzian line shapes were used. Normalized least-squares residuals were calculated by $[\sum(y_i - f_i)^2]^{1/2}/y_{max}$, where y_i are the experimental data, f_i are the fit values, and y_{max} is the data maximum amplitude. Local minima in the least-squares fit (alternate solutions) were found by systematically varying the input, first-guess parameters. The fits determined the amplitudes $A_{x,y,b}$ and $D_{x,y,b}$. From D_x and D_y the angles between the A_x and A_y transition moments and the gel squeezing axis (membrane normal) were calculated. Tilt of the heme normal from the orientation axis was then determined by assuming that the A_x and A_y directions are orthogonal and lie in the heme plane.

RESULTS

Orientation of Reaction Center in Squeezed Polyacrylamide Gels. Reaction centers vesicles were oriented in an aqueous environment with squeezed polyacrylamide gels. The extent of reaction center orientation was assayed by measurement of the dichroism for the bacteriochlorophyll dimer, B_2, Q_y (860 nm) and Q_x (600 nm) transitions. Previous dichroism measurements (Vermeglio & Clayton, 1976; Rafferty & Clayton, 1979) showed that in the natural membrane the 860-nm transition is oriented nearly parallel to the membrane surface, while the 600-nm transition is tilted out of plane.

Dichroism of the light-induced loss of the 860- and 600-nm absorptions accompanying the generation of the $B_2^+Q^-$ state

Table I: Bacteriochlorophyll Dimer Orientation in Squeezed Polyacrylamide Gels

transition (nm)	S	θ (deg)	S_T	θ_T (deg)[a]	S_M
860	−0.29 ± 0.05	68 ± 3.5	−0.36 ± 0.02	72 ± 1	0.80 ± 0.2
600	0.38 ± 0.02	40 ± 1	0.41 ± 0.35	39 ± 15	0.93 ± 0.46

[a] Determined by Rafferty & Clayton (1979).

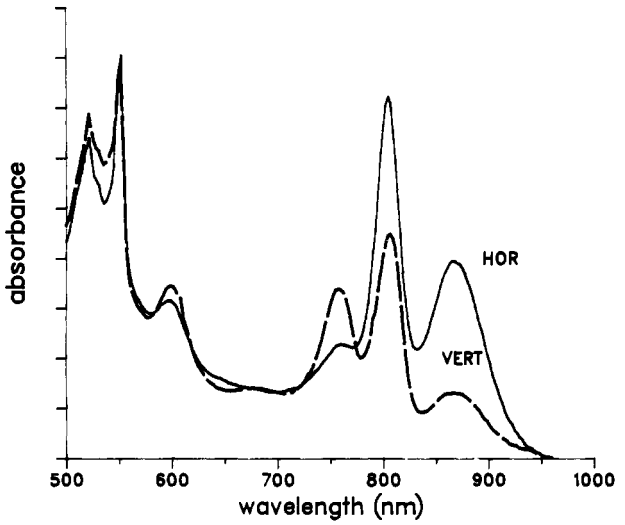

FIGURE 3: Absorption spectra of reaction center vesicles measured with linearly polarized light in squeezed polyacrylamide gels. The solid line spectrum was measured with the electric vector of the polarized light perpendicular to the gel squeezing axis, A_H, and the dashed line spectrum measured with the electric vector parallel to this axis, A_V. The reaction center concentration was 2.5 μM. The cytochrome c_2 (25 μM) was reduced by soaking the gels in 1 mM ascorbate.

are shown in Figure 2, for oriented reaction center vesicles in the presence of ferricyt c. The largest absorption change for the 860-nm transition is seen with light polarized perpendicular to the gel squeezing axis, ΔA_H. Conversely, the largest 600-nm absorption change is seen with light polarized parallel to the gel squeezing axis, ΔA_V. Since membranes are expected to align with the membrane normal along the gel compression axis (see Material and Methods), these results indicate that the 860-nm transition lies approximately parallel to the membrane surface, while the 600-nm transition points out of plane. For different samples, dichroic ratios $(\Delta A_V - \Delta A_H)/\Delta A$ were found to be in the range −0.87 ± 0.2 for the 860-nm absorption transient and 1.14 ± 0.1 for the 600-nm change. These dichroic ratios correspond to angles, θ, of 68° ± 3.5° and 40° ± 1° for the 860- and 600-nm transitions, respectively (Table I). This dichroism for reaction center membranes is also evident in the polarized absorption spectra, shown in Figure 3 for a sample with ferrocyt c_2. These spectra show the 860-nm transition to absorb more strongly with light polarized in the plane of the membrane, as does the 800-nm absorption, while the 760-nm Q_y transitions of the reaction center bacteriopheophytins preferentially absorb light polarized along the membrane normal.

The dichroism spectra shown here are analogous to those reported previously for reaction centers in the chromatophore membrane (Rafferty & Clayton, 1979; Vermeglio & Clayton, 1976). Rafferty and Clayton (1979) calculated the angles θ_T between the membrane normal and the 860- and 600-nm transitions to be 72° ± 1° and 39° ± 15°, respectively. The correspondences between the angles θ measured here between the optical transitions and the gel orientation axis and the calculated angles θ_T with the membrane normal (Table I) indicate that the reaction centers are very well ordered in the squeezed acrylamide gels. Membrane orientation parameters,

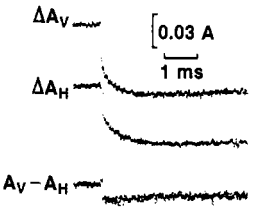

FIGURE 4: Light-induced cytochrome c_2 oxidation by reaction center vesicles in squeezed polyacrylamide gels. The traces are 550-nm − 540-nm differences for single-beam transients, averaged 8 times and measured with linearly polarized light. The reaction center concentration was 5.1 μM. The total, unpolarized absorption change was $-0.0476\Delta A$, corresponding to a cytochrome concentration of 2.38 μM. This is 47% of the total reaction center concentration, suggesting, as discussed under Materials and Methods, that the quinone acceptor accumulates in the reduced state in the remainder of the reaction centers and prevents photochemistry.

S_M, are calculated to be 0.80 ± 0.2 and 0.93 ± 0.46 from the 860- and 600-nm dichroism data, respectively. As discussed under Materials and Methods, S_M varies from a value of 0 for a random distribution to 1 for a complete alignment. Because of the high degree of orientation induced with the reaction center vesicles, the following cytochrome dichroism data were not corrected for membrane disorder.

Dichroism of Cytochrome c_2–Reaction Center Complexes. (*A*) *Kinetic Dichroism Measurements.* In the presence of ferrocyt c_2, flash excitation of the reaction center generates the $cB_2^+Q^-$ redox state, which subsequently oxidizes one cyt c_2 per reaction center: $c^+B_2Q^-$. Figure 4 shows the light-induced 550–540-nm absorbance transients accompanying cyt c_2 oxidation in squeezed polyacrylamide gels and measured with linearly polarized light. The transients are found to be biphasic with 5 μM reaction center and 20 μM cyt c_2. The fast phase (τ = 1–3 μs; Overfield et al., 1979; Overfield & Wraight, 1980; Rosen et al., 1980) could not be resolved with the 10-μs response of the instrument, but semilog plots fit the A_V and A_H slow phases with single, first-order decays with half-times of 220 μs (τ = 317 μs) and 275 μs (τ = 397 μs), respectively. The extrapolation of the semilog plots to zero time shows that extents of the slow phase oxidations are the same for both A_V and A_H polarizations. However, the fast oxidation component shows a larger absorption change measured with light polarized along the A_V direction. The dichroism of the fast phase is also evident in the $\Delta A_V - \Delta A_H$ difference kinetic trace (Figure 4). The proportion of fast-phase oxidation varied in the range 40–60% for different preparations, and the dichroism that was only seen in the fast phase varied in the range $(\Delta A_V - \Delta A_H)/\Delta A = 0.45 \pm 0.05$ at 550 nm.

A spectrum of the fast phase component of the flash-induced absorbance changes is shown in Figure 5 with the filled circles. The top spectrum shows the unpolarized absorbance changes. The solid line is a chemically reduced minus oxidized difference spectrum generated with isolated cyt c_2 in 10 mM Tris, pH 7.8, and normalized to the 550-nm absorbance transient. The middle spectrum, filled circles, is the $\Delta A_V - \Delta A_H$ dichroism due to the fast kinetic phase. The solid line is the total cyt c_2 dichroism, $A_V - A_H$, measured from the total cyt c_2 absorbance in the oriented membrane sample, which is described in the following section. The bottom trace in Figure 5 shows

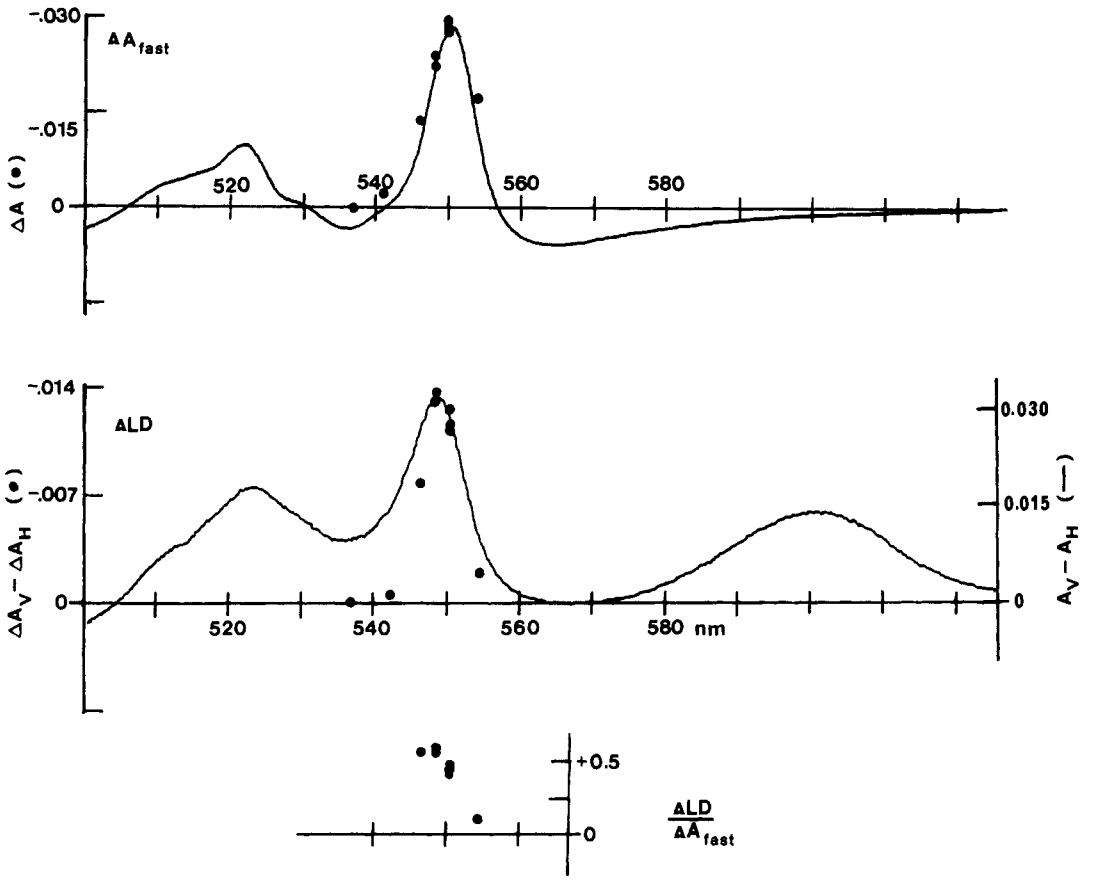

FIGURE 5: Linear dichroism ($A_V - A_H$) for cytochrome c_2 when bound to reaction center vesicles in squeezed polyacrylamide gels. (Top) The top traces show unpolarized spectra. The solid circles mark the light-induced absorbance changes due to the fast-oxidation phase of cytochrome c_2 in gels. The solid line is a chemically oxidized minus reduced difference spectrum. (Middle) The middle traces are the corresponding linear dichroism difference spectra for cytochrome c_2 bound to the reaction center vesicles. The solid circles are the kinetic differences, $\Delta A_V - \Delta A_H$, between the absorption transients measured with vertially and horizontally polarized light. Differences are only seen for the fast component of the oxidation kinetics. The solid line is the linear dichroism spectrum, $A_V - A_H$, determined by taking the difference between "static" spectra measured with vertically and horizontally polarized light. The spectrum was obtained by recording the linear dichroism spectrum for the oriented reaction center vesicles plus cytochrome c_2 and subtracting the dichroism obtained for reaction center vesicles alone. (Bottom) Spectrum of the kinetic dichroic ratio, $(\Delta A_V - \Delta A_H)/\Delta A$, for the fast component of the cytochrome c_2 oxidation. The reaction center and cytochrome c_2 concentrations were 5 and 20 μM, respectively. The same dichroic ratio found for the kinetic measurements can be calculated from the absorption dichroism by dividing $A_V - A_H$ by a cytochrome c_2 absorption corrresponding to the percent fast phase times the total reaction center concentration. This indicates that all of the absorption dichroism can be accounted for by the cytochrome c_2 population that undergoes rapid oxidation. The difference in absolute extent of the kinetic and absorption dichroism in the middle spectra is a reflection of the fact that only a portion (~50%) of the reaction centers were repeatablely flash activatable. As discussed in Figure 4 and under Materials and Methods, this is apparently due to accumulation of the quinone acceptor in the reduced state.

the wavelength dependence of the kinetic dichroic ratio ($\Delta A_V - \Delta A_H)/\Delta A$ calculated for the fast phase of the cyt c_2 oxidation. The peak of the kinetic dichroism spectrum was seen to be shifted 0.5–1.0 nm to shorter wavelengths from that of the unpolarized spectrum.

(*B*) *Total Cyt c_2 Dichroism.* The kinetic dichroism measurements are sensitive only to cytochromes bound to oxidation sites on the reaction center protein. A measure of the total dichroism arising from all oriented cytochromes can be obtained by measurement of the dichroism for the full cytochrome c_2 absorption. An absorbance dichroism spectra, $A_V - A_H$, for cyt c_2 was obtained by recording the linear dichroism spectrum for reaction center reconstituted vesicles plus cyt c_2 and subtracting the dichroism obtained for the reaction center reconstituted vesicles alone, after having normalized the spectra for the dichroism of the reaction center by the bacteriopheophytin peak at 760 nm. This difference is the solid line trace in the middle spectrum in Figure 5. The reaction center concentration was 5 μM and cyt c_2 concentration was 25 μM. The dichroism spectrum is similar to the absorption spectrum, although the peak position is shifted 0.5–1.0 nm to shorter wavelengths.

The cyt c_2 absorbance dichroism will have a contribution due to the population of cytochrome that is bound to the reaction center and gives rise to the fast oxidation (~0.5 cyt/RC), plus the dichroism of other populations of oriented cyt c_2. The total dichroism for cyt c_2 at 550 nm with 5 μM reaction center is 0.0275 ± 0.01. Dividing this value by the absorption due to the rapidly oxidized cyt c_2 population (2.5 μM) yields a dichroic ratio $(A_V - A_H)/A$ of 0.4 ± 0.02. This value matches closely that determined at 550–540 nm (0.45 ± 0.05) for the rapid phase of the flash-induced absorbance changes. This equivalence demonstrates that the cytochrome population that undergoes rapid oxidation can account for the entire cyt c_2 dichroism.

The correspondence between the cyt c_2 absorbance dichroism and the rapid kinetic phase can be seen in a titration of the reaction center reconstituted vesicles with cyt c_2. Figure 6A shows the cyt c_2 absorbance dichroism at 550 nm (solid circles) and the percent fast-phase oxidation (open circles) measured as a function of cyt c_2 concentration with reaction center vesicles having a reaction center concentration of 0.8 μM. The solid line is a calculated curve with a dissociation constant of 6 μM. The similarity of the extent of dichroism and the

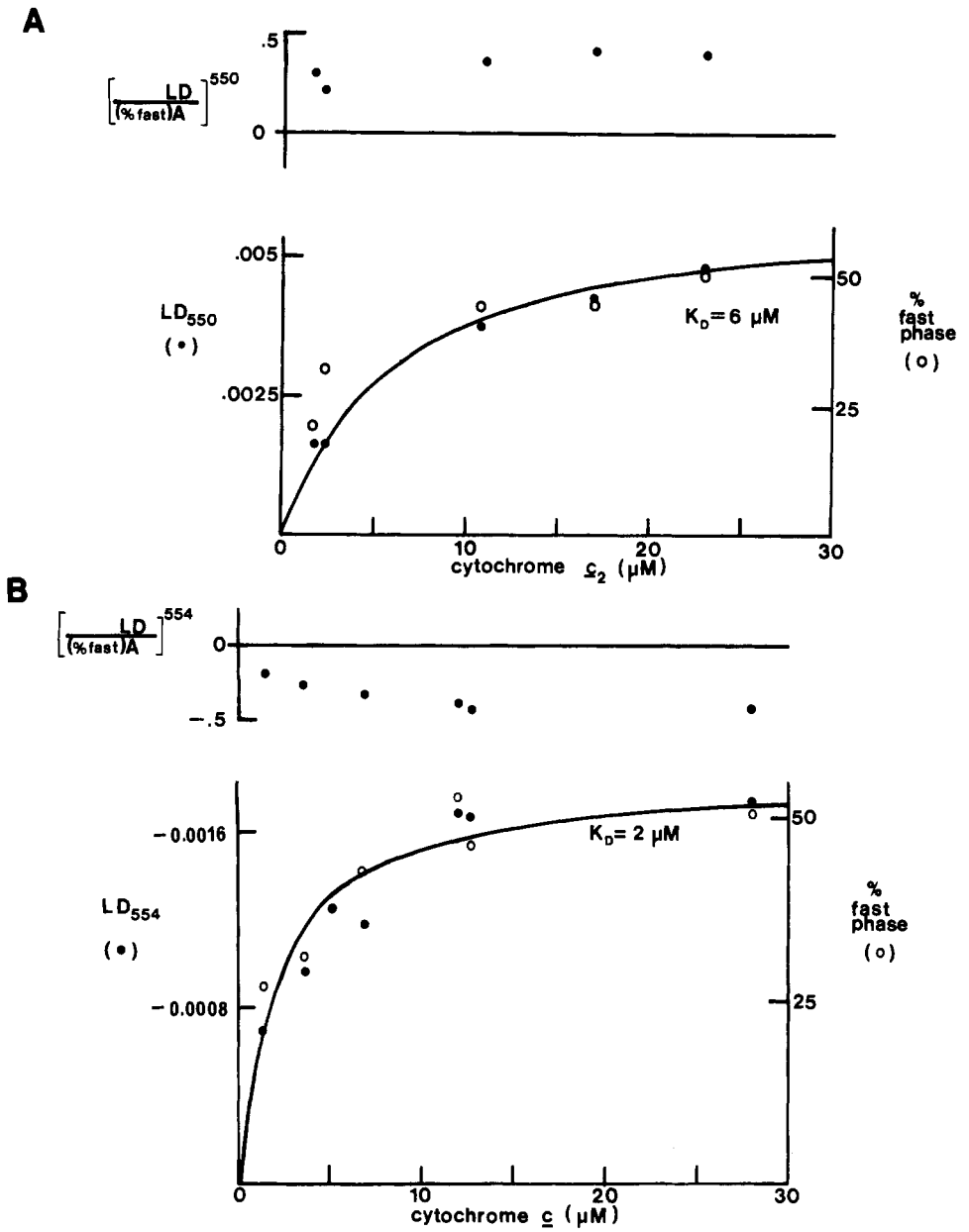

FIGURE 6: Titration of reaction center vesicles with cytochrome c and c_2 in squeezed polyacrylamide gels. (A) Titration with cytochrome c_2 and a reaction center concentration of 0.8 μM. The filled and open circles show the concentration dependence for the absorption dichroism $A_V - A_H$, measured at 550 nm, and the extent of the rapid cytochrome c_2 oxidation, respectively. The solid line is a calculated binding curve with a dissociation constant of 6 μM. The upper portion of part A shows the dependence of the dichroic ratio on cytochrome c_2 concentration, calculated by dividing the linear dichroism $A_V - A_H$ measured at 550 nm by the absorption due to the portion of the cytochrome population that undergoes rapid oxidation. (B) Titration with cytochrome c and a reaction center concentration of 0.55 μM. The filled and open circles show the dependencies on cytochrome c concentration for the absorption dichroism $A_V - A_H$ measured at 554 nm and the extent of rapid cytochrome c oxidation, respectively. The solid line is a calculated binding curve with a 2 μM dissociation constant.

percent fast phase support the conclusion that only the cyt c_2 population that gives rise to the rapid oxidation phase is dichroic.

These dichroism data find that with reaction centers reconstituted into phosphatidylcholine membranes there is only one dichroic binding site for cyt c_2, which has at saturation a stoichiometry of 0.5 cyt c_2 per reaction center. The cytochrome population that is associated with the slow oxidation phase must either be bound in a nondichroic fashion (i.e., with the heme normal at 55° to the membrane normal or bound randomly) or may be due to a diffusion-limited reaction between unbound cyt c_2 and the reaction center.

Dichroism of Reaction Center–Cytochrome c Complexes. (A) Kinetic Dichroism Measurements. The dichroism of the reaction center–cyt c_2 complex can be compared to that of the reaction center–cyt c complex. Flash-induced oxidation of the reaction center is also seen to initiate biphasic oxidation of the cyt c; however, the fast oxidation phase is ~10-fold slower than that with cyt c_2 (Overfield et al., 1979; Overfield & Wraight, 1980; Rosen et al., 1980). In contrast to the dichroism for cyt c_2 oxidation that was always positive ($\Delta A_V > \Delta A_H$), the dichroism for the flash-induced cyt c oxidation was found to be close to zero near the absorbance maximum at 550 nm but increased on either side of this peak with a dichroism of opposite sign. The top trace in Figure 7 shows a plot of the unpolarized light induced absorption changes (solid circles), and a plot of the polarized $\Delta A_V - \Delta A_H$ difference spectrum is shown in the middle trace (solid circles). The bottom trace shows a plot of the kinetic dichroic ratio, determined by dividing the extent of the kinetic dichroism ($\Delta A_V - \Delta A_H$) by the unpolarized absorption change due to the fast phase (50% ΔA_{total}), which varied from 0.3 ± 0.2 at 546–540

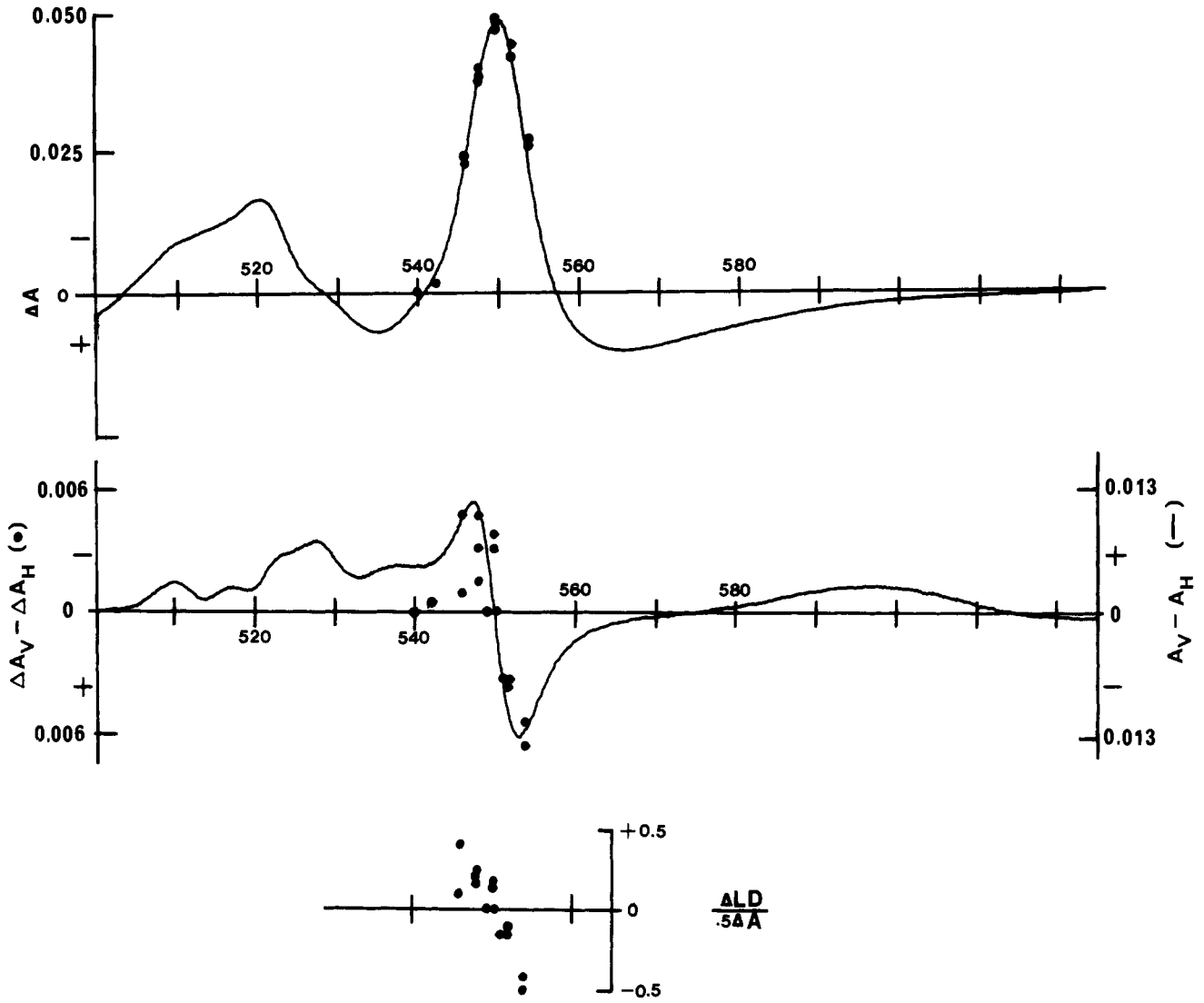

FIGURE 7: Linear dichroism spectra for cytochrome *c* bound to reaction center vesicles in squeezed polyacrylamide gels. The spectra are analogous to those in Figure 6. (Top) The top traces are unpolarized spectra. The solid circles mark the total flash-induced absorption changes (fast plus slow phases) for cytochrome *c* in these gels. The solid line is the chemically oxidized minus reduced spectrum. (Middle) The middle traces show the linear dichroism spectra for cytochrome *c* bound to the reaction center vesicles. The solid circles are the $\Delta A_V - \Delta A_H$ differences for the flash-induced cytochrome *c* absorption transients measured with linearly polarized light. The solid line is the absorption dichroism, $A_V - A_H$, obtained by measuring the dichroism spectrum for gels containing reaction center vesicles plus cytochrome *c* and subtracting the dichroism obtained from gels containing reaction center vesicles alone. (Bottom) Spectrum of the dichroic ratio $(\Delta A_V - \Delta A_H)/\Delta A$, associated with the fast phase of the cytochrome oxidation kinetics. Comparable values can be calculated from the "static" dichroism spectrum, $A_V - A_H$, by dividing by the absorption of the cytochrome *c* population that undergoes rapid oxidation. The reaction center and cytochrome *c* concentrations were 4 and 20 μM, respectively.

nm to −0.5 ± 0.1 at 554–540 nm.

(*B*) *Total Cytochrome c Dichroism.* The total absorbance dichroism for cyt *c* in association with the reaction center–phosphatidylcholine membranes was determined as above, by recording the absorption dichroism for a sample of reaction center membranes plus cyt *c* and subtracting the dichroism from the reaction center vesicles alone. The resulting cyt *c* dichroism spectrum $A_V - A_H$ is shown by the solid line trace in the middle spectrum of Figure 7. The cyt *c* kinetic and absorption dichroism spectra are similar, both having a dichroism of opposite sign on either side of the unpolarized absorption maximum. These cyt *c* dichroism spectra differ markedly from the spectra seen for the reaction center–cyt c_2 complex. The splitting of the cytochrome *c* dichroism spectrum suggests that the 550-nm absorption band is composed of two overlapping components that have dichroisms of opposite sign.

The correspondence between the fast oxidation phase and the absorbance dichroism is shown by a titration of the reaction center vesicles having a reaction center concentration of 0.55 μM, with cytochrome *c* (Figure 6B). Both the dichroism $A_V - A_H$ and the extent of fast-phase oxidation show a similar dependence on cyt *c* concentration. The solid line is calculated curve with a dissociation constant of 2 μM. A dichroic ratio calculated by dividing the dichroism $A_V - A_H$ at 554 nm by the absorption due to the population of cyt *c* that undergoes fast oxidation yields a value −0.41 ± 0.7. The similarity between this value and that measured in the kinetic experiment indicates, as in the case of cyt c_2, that the cyt *c* that is bound to the reaction center and gives rise to the fast oxidation accounts for the entire cyt *c* dichroism. This suggests that there is only one dichroic binding site for cyt *c* on the reaction center membranes, which has a stoichiometry of 0.5 cyt *c* per reaction center. However, the qualitatively different linear dichroism spectra for cyt *c* and c_2 suggest that heme orientation differs in each case.

Dichroism of Cytochrome c Bound to Negatively Charged Membranes. In addition to binding to protein sites, cyto-

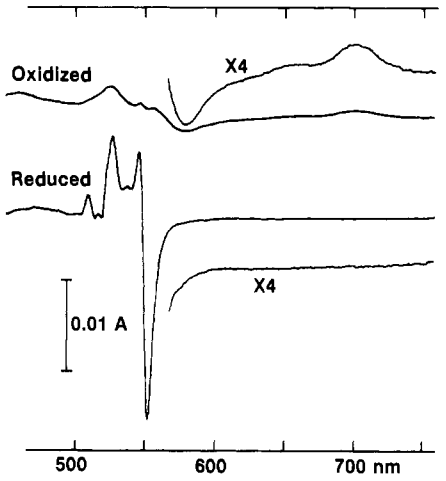

FIGURE 8: Absorbance dichroism spectrum, $A_V - A_H$, for oxidized and reduced cytochrome *c* bound to negatively charged vesicles and oriented in squeezed polyacrylamide gels. Vesicles with a total lipid concentration of 0.6 μM were composed of phosphatidylcholine and phosphatidylinostitol in a 5:1 ratio. The cytochrome *c* concentration was 28 μM. The reduced sample was soaked in 1 mM sodium ascorbate. The insets show a 4 times expanded vertical scale.

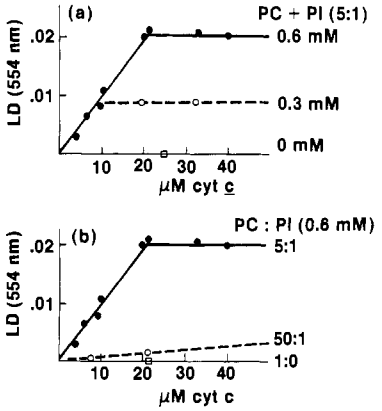

FIGURE 9: Titrations of dichroism signal for ferrocytochrome *c* bound to lipid vesicles with varying lipid compositions in squeezed polyacrylamide gels. Part a shows that the maximal dichroism signal is proportional to the concentration of charged vesicles. The cytochrome dichroism as a function of cytochrome concentration is plotted for samples having a constant 5:1 phosphatidylcholine to phosphatidylinostitol ratio, but with total lipid concentrations of 0.6 mM (●), 0.3 mM (○) and no lipid (□). Part b shows titrations with a constant total lipid concentration (0.6 mM), but with varying phosphatidylcholine to phosphatidylinostitol ratios: (●) repeats the 5:1 ratio from part a, (○) 50:1 ratio, and (□) pure phosphatidylcholine vesicles. The titrations show that the cytochrome *c* dichroism signal arises from a specific binding to negatively charged vesicles and is not due to artifactual associations between cytochrome *c* and the polyacrylamide gel.

chrome *c* also binds electrostatically to the surface of negatively charged membranes (Das et al., 1965; Fromherz, 1970; Steinemann & Lauger, 1971). A dichroism signal is seen for cytochrome *c* bound to negatively charged vesicles and oriented in the squeezed polyacrylamide gels. Figure 8 shows the absorbance dichroism spectrum measured for oxidized and reduced cytochrome *c* bound to vesicles composed of phosphatidylcholine (PC) plus phosphatidylinositol (PI) in a 5:1 ratio. The dichroism of the membrane-bound cytochrome is qualitatively similar to that seen for the reaction center–cyt *c* complex but differs in the relative ratio of the positive and negative components. In addition, the extent of the dichroism per bound cytochrome is smaller than in the case of the cytochrome *c*–reaction center complex. The number of cytochromes bound to the charged vesicles can be estimated from titrations of the vesicles with cytochrome *c*.

Figure 9a shows the amplitude of the dichroism measured as a function of cytochrome *c* concentration, with vesicles composed of PC + PI in a 5:1 ratio. With 0.6 mM total lipid, the extent of dichroism saturates near 20 μM cytochrome *c*. The nonhyperbolic form of the titration suggests that stoichiometric binding occurs until saturation is reached. This result is consistent with the 1.1 μM dissociation constant measured for cytochrome *c* binding to mixed, negatively charged vesicles (Teissie, 1981) and a much higher concentration of binding "sites" provided by the 0.1 mM PI. Dividing the dichroism amplitude at 553 nm by the absorbance of the 20 μM bound cyt *c* yields a dichroic ratio of −0.047 for this population. This value is approximately 10-fold smaller than the dichroism seen for the reaction center–cyt *c* complex.

Figure 9a also shows that the maximal extent of the cyt *c* dichroism signal is dependent upon the concentration of vesicles. Halving the total vesicle concentration while holding the PC:PI ratio constant diminishes the dichroism by a factor of approximately 2. In the absence of mixed PC + PI vesicles, the absorption spectrum of cytochrome *c* is not dichroic in the squeezed polyacrylamide gels. Figure 9b shows the effect of varying the PC:PI ratio while holding the total lipid concentration constant (0.6 mM). With pure PC vesicles, the cytochrome *c* does not show an absorption dichroism. The absence of dichroic binding sites on the PC membrane is also consistent with the measurements on reaction centers reconstituted into PC vesicles, where only the reaction center binding sites were found to be dichroic. At a PC:PI ratio of 50:1 a small dichroism is seen for cyt *c*. The top trace repeats the data for the 5:1 PC:PI ratio. These experiments show that a dichroic binding of cytochrome *c* to vesicles only occurs with negatively charged membranes. These experiments rule out the possibility that the dichroism arises from artifacts due to associations between cytochrome *c* and the acrylamide gel.

Analysis of Cytochrome Dichroism Spectra. Figures 5, 7, and 8 show that the dichroic ratios for cyt *c* and c_2 bound to the reaction center and for cyt *c* bound to negatively charged vesicles are not constant throughout the α-band absorption. This will occur if the α-band is composed of more than one component with different dichroic ratios. Dichroism studies on cytochrome *c* single crystals (Eaton & Hochstrasser, 1967) and in polyvinyl alcohol films (Vermeglio et al., 1980) have suggested that optical absorptions in the heme *x* and *y* directions are not completely degenerate. Low-temperature absorption spectra of ferrocyt *c* and c_2 in 60% glycerol confirm this (top spectra of Figures 10 and 11) and show the α-band to split into two components. This suggests that the room temperature absorption and dichroism spectra can be analyzed as the sum of two overlapping components. As described under Materials and Methods, fits to the low-temperature spectra were used to determine the integrated intensity for each component. By holding these intensities constant, simultaneous fits to the room temperature absorption and dichroism spectra were used to determine the position of these components at room temperature and the sign and amplitude of their dichroism.

The low-temperature absorption spectra of cyt *c* and c_2 (top spectra of Figures 10 and 11) could be fit very closely as the sum of three Lorentzian components, A_x, A_y, and A_b, where A_x and A_y are the two α-band components, defined as the short- and long-wavelength components, respectively, and A_b arises from the adjacent β-band. The solid-line fits are essentially superimposable on the experimental 100 K spectra (dashed lines). The normalized least-squares residuals were <0.1 for each cytochrome. A tabulation of the positions and

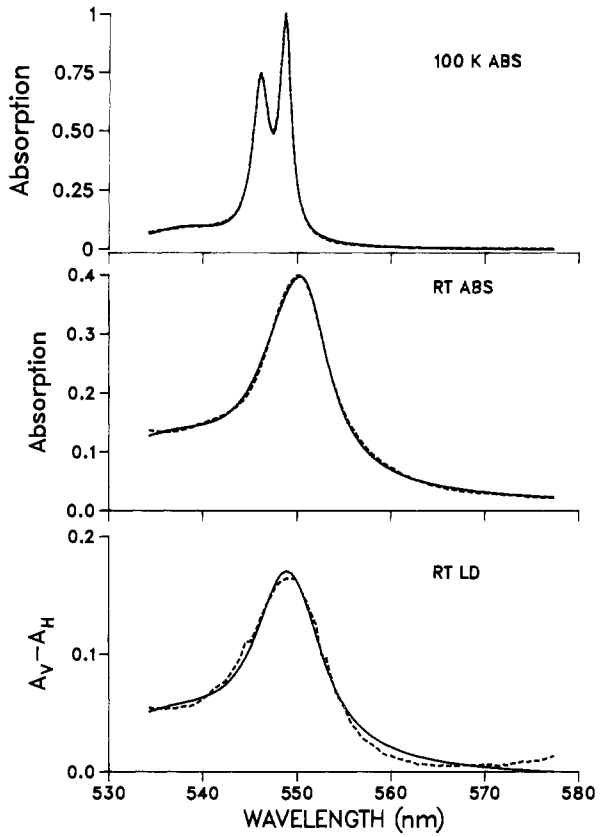

FIGURE 10: Simulation of cytochrome c_2 absorption and dichroism spectra. (Top) The dotted line is the experimental absorption spectrum for cytochrome c_2 at 100 K in 65% glycerol and 35% 10 mM Tris, pH 8. The solid line is the sum of three Lorentzian components fit to the experimental spectra. The fit parameters are summarized in Table II. (Middle) The dotted line is the experimental absorption spectrum for cytochrome c_2 at room temperature. The solid line is the fit obtained by simultaneously fitting the room temperature absorption and dichroism spectra as the sum of three Lorentzian components. (Bottom) The dotted line is the experimental dichroism spectrum ($A_V - A_H$) measured for cytochrome c_2 bound to reaction center vesicles as described in Figure 6, middle trace. The solid line is the fit obtained by simultaneously fitting the absorption and dichroism spectra as the sum of three Lorentzian components, as described in the text and under Materials and Methods.

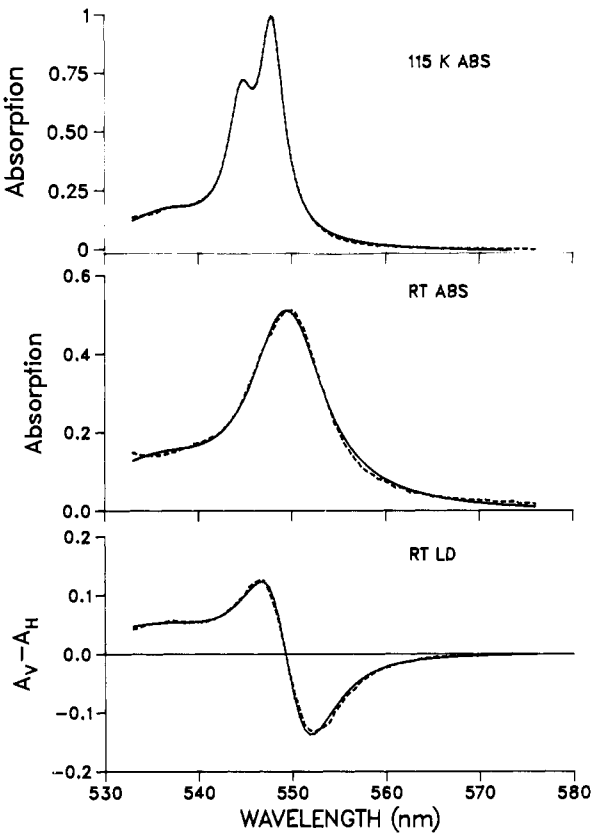

FIGURE 11: Simulation of cytochrome c absorption and dichroism spectra. (Top) The dotted line is the experimental absorption spectrum for cytochrome c at 115 K in 65% glycerol and 35% 10 mM Tris, pH 8. The solid line is the sum of three Lorentzian components fit to the experimental spectra. The fit parameters are summarized in Table II. (Middle) The dotted line is the experimental absorption spectrum for cytochrome c at room temperature. The solid line is the fit obtained by simultaneously fitting the room temperature absorption and dichroism spectra as the sum of three Lorentzian components. (Bottom) The dotted line is the experimental dichroism spectrum ($A_V - A_H$) measured for cytochrome c bound to reaction center vesicles as described in Figure 7, middle spectrum. The solid line is the fit obtained by simultaneously fitting the absorption and dichroism spectra as the sum of three Lorentzian components, as described in the text and under Materials and Methods.

Table II: Line-Shape Parameters Derived from Fits to α-Band Absorption and Dichroism Spectra

complex	absorption component	peak position (nm)	half-width at half-height (nm)	relative area
RC–c_2	A_y	551.1	3.16	0.91
	A_x	548.8	4.28	1.0
RC–c	A_y	550.8	4.37	1.0
	A_x	548.8	4.11	0.66
vesicle–c	A_y	550.9	4.32	1.0
	A_x	548.8	4.09	0.67

line widths determined by these fits for cytochrome c and c_2 is given in Table II.

A simultaneous fit to the cytochrome c_2 room temperature absorption (middle spectrum, Figure 10) and dichroism due to the reaction center bound cytochrome (lower spectrum, Figure 11) yielded a least-squares residual of 0.277. The resulting positions and line widths for the A_x and A_y components at room temperature are also listed in Table II. The fit yielded dichroic ratios of 0.827 and 0.132 for these components, which correspond to angles of 44.0° and 53.0° between the A_x and A_y transitions and the membrane normal. By assuming that these components are orthogonal and lie in the plane of the heme, the angle between the normal to the heme and the membrane normal can be calculated from the vector cross product to be 69.7° (Table III).

Table III: Orientation of Heme Normal and Q_x and Q_y Directions

complex	θ_x (deg)	θ_y (deg)	θ_n (deg)
RC–c_2	44.0	53.0	69.7
RC–c	28.8	83.4	62.2
vesicle–c	57.0	52.3	55.0

Two acceptable fits (least-squares residuals ≤ 0.25) were found for the spectra of cytochrome c bound to the reaction center. One set occurred when the positions of the A_x and A_y components were nearly overlapping (peak separation ≤ 0.9 nm). This set of solutions was rejected since it required A_x and A_y to have dichroisms that exceed the physically possible bounds (i.e., $3 \geq LD/A \geq 1.5$). The other solution (middle spectrum, Figure 11) occurred with A_x and A_y peak separations of 2.0 nm. This solution required A_x and A_y to have dichroic ratios of 1.96 and −1.44, respectively, which correspond to tilts of 28.8° and 83.4° from the membrane normal. These values yield an angle of 62.2° between the heme normal and the membrane normal (Table III).

For cytochrome c bound to negatively charged membranes, dichroism spectra were measured in both the heme oxidized and reduced states. The dichroism spectrum for the oxidized cytochrome shows a component at 695 nm. This transition

has been assigned to an π–d_{z^2} (Fe^{III}) transition polarized perpendicular to the plane of the heme (Gouterman, 1978; Eaton & Hochstrasser, 1967). Hence, the dichroism of this transition provides a direct measure of the angle between the heme and membrane normals and can be compared to the tilt calculated from the fits to the dichroism for the reduced cytochrome.

The sign of the 695-nm dichroism suggests that the angle between the oxidized heme normal and the membrane normal is <54.7° (i.e., $A_V > A_H$). By use of an extinction coefficient of 840 M^{-1} cm^{-1} (Eaton & Hochstrasser, 1967), a dichroic ratio of 0.041 is calculated for the 695-nm band, which corresponds to an angle of 54.2° between the heme and membrane normals.

Fits to the dichroism spectrum of the reduced cytochrome bound to negatively charged vesicles were performed as described above. One solution gave positions and amplitudes for the A_x and A_y components that are nearly identical with those found to fit the cytochrome *c*–reaction center dichroism (Table II). This fit to the cytochrome *c*–vesicle dichroism gave tilt angles of 52.3° and 57.0° for the A_x and A_y components, corresponding to a 55.0° angle between the heme and membrane normals. This fit for the reduced cytochrome predicts that the 695-nm transition of the oxidized cytochrome should show a small dichroism of opposite sign from that observed. However, differences could arise if the reduced and oxidized cytochromes were not bound with identical orientations or if the assumptions on the positions of the A_x, A_y, and 695-nm transitions with respect to the heme axes were slightly in error. The agreement within 2° for the heme orientation measured from the 695-nm band and derived from fits to the dichroism spectrum of the reduced cytochrome suggests that the procedures used for fitting are appropriate. The other fit to the reduced heme spectra gave an angle of 53.4° between the heme and the membrane normals, but this solution was rejected since it required amplitudes and line widths for the A_x and A_y components that could not be used to fit the dichroism spectra of the cytochrome bound to the reaction center.

Discussion

"Proximal" and "Distal" Binding Configurations. Previous kinetic studies have suggested that two types of *c* cytochrome–reaction center complexes can be formed. They are distinguished by their rapid or slow rates of oxidation (Dutton et al., 1976; Overfield et al., 1979; Moser & Dutton, 1986). Notations of proximal and distal configurations have been used to imply that differences in cytochrome orientation could account for these kinetic differences (Dutton & Prince, 1978; Moser & Dutton, 1986). The dichroism measurements reported here show that, in fact, heme orientations for the two populations are physically distinct. Only the fast-phase cytochrome oxidation is seen to be dichroic. Significantly, the linear dichroism spectra for cytochrome *c* and c_2 bound to the reaction center are qualitatively different, indicating that heme orientation differs in each case. This may be in part responsible for the 20-fold difference in oxidation rate. As described below, the dichroism spectra for cytochrome *c* and c_2 can be interpreted to arise from binding involving the protein surface near to the exposed heme edge.

The slow phase has also been attributed to arise from a diffusion-limited reaction with cytochrome *c* in solution (Rosen et al., 1979). The present dichroism data cannot distinguish this possibility from that of a bound, but weakly dichroic cytochrome population. For example, the dichroism of cytochrome *c* bound to the negatively charged membrane is sufficiently small that it would not be discerned with the present signal-to-noise in binding experiments with the reaction center. A cytochrome bound rigidly with the A_x and A_y transitions oriented near 55° to the membrane normal would be nondichroic, as would a bound, but rotating cytochrome whose A_x and A_y directions have on average nearly equal projections perpendicular and parallel to the membrane.

Dichroic Binding Surfaces on Cytochromes c and c_2. The dichroism data find that in the cyt c_2–reaction center complex the heme is tilted 7.5° more perpendicular to the membrane and rotated by 32° about the heme normal compared to the cyt *c*–reaction center complex. If the placements of the optical transition moments with respect to the molecular axes are known, then dichroism data can be used to identify molecular orientation. The Soret and α-band absorptions are known to lie in the plane of the heme (Eaton & Hochstrasser, 1967; Hofrichter & Eaton, 1976), but their directions in the plane are not known. This means that the observed cytochrome dichroism limits possible sites for binding to specific circumferences on the cytochrome surface. However, likely locations for the optical *x* and *y* directions are restricted by the symmetry of the heme, which suggests that the *x* and *y* directions may lie along the Fe–pyrrole ring directions (Gouterman, 1978; Adar, 1978), and by the likelihood that the most efficient electron transfer will occur via the exposed heme edge.

For example, by assignment of A_y to the pyrrole ring D (with the surface-exposed propionic acid side chain) to pyrrole ring B (bound to cysteine-14) direction [see Takano and Dicherson (1981) for nomenclature] and A_x to the pyrrole C (bound to cysteine-17) to pyrrole A (with the buried propionic acid) direction, the crystal structure of cytochrome c_2 can be rotated so that A_x and A_y directions make projections on the membrane normal as described in Table III for the cyt c_2–reaction center complex. This causes the cytochrome surface shown in Figure 12a to be in direct contact with the reaction center binding site. The view in Figure 12 is out from the membrane along the membrane normal. The orientation of cytochrome c_2 places the exposed heme edge squarely facing the reaction center. Neither of the Fe–pyrrole ring directions are facing the binding site. The long protein segment 95–105 lies closest to the reaction center site. This segment is remarkably rich in lysine residues, at positions 95, 97, 99, 103, 105, and 106, which are labeled in Figure 12A. It is suggested that these residues dominate the binding interactions for the rapidly oxidized cytochrome c_2 population. The phenylalanine-102 is positioned where it may form hydrophic contacts with the reaction center but may not be involved in the electron transfer from the heme to bacteriochlorophyll.

This orientation for cytochrome c_2 is consistant with the structure of the cytochrome binding site on the reaction center. Chemical cross-linking and antibody labeling has shown that this site is composed of the reaction center L and M subunits on the extracellular surface of the membrane (Rosen et al., 1983). Crystal structures of the *R. sphaeroides* (Chang et al., 1986) and *Rhodopseudomonas viridis* (Deisenhofer et al., 1985) reaction centers show that this surface is parallel to the surface of the membrane. The cytochrome c_2 orientation in Figure 12A permits the closest approach of heme to the bacteriochlorophyll dimer acceptor.

The orientation of the cytochrome c_2 heme in Figure 12A, including the positions of the Fe–pyrrole directions, is very similar to that for the heme closest to the bacteriochlorophyll dimer in the cytochrome subunit of the *Rp. viridis* reaction center (Deisenhofer at al., 1985). The optical dichroism for the *Rp. viridis* cytochrome (Vermegelio et al., 1980) is analogous to that seen here for cytochrome c_2 bound to the

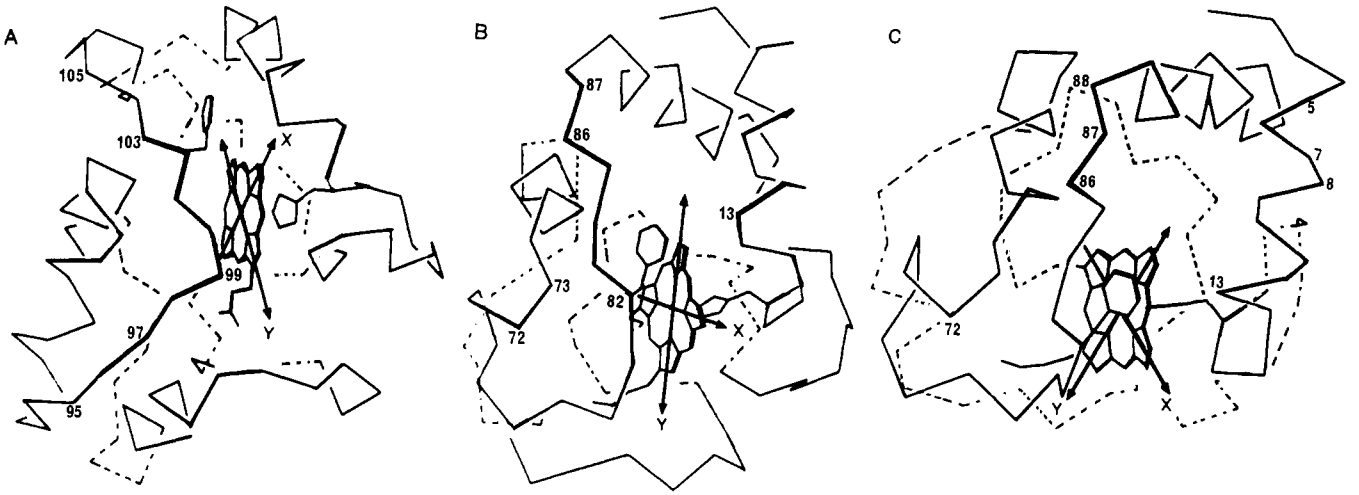

FIGURE 12: Orientations for bound cytochrome c and c_2 determined from dichroism measurements. The view in each case is out from the membrane along the membrane normal. The cytochrome structures have been rotated so that the heme x and y directions (see text) make projections on the membrane normal as determined for the A_x and A_y transitions (Table III). (A) The cytochrome c_2–reaction center electron-transfer complex. The figure shows the protein backbone for *Rhodospirillium rubrum* cytochrome c_2 (Brookhaven National Laboratory Protein Data Bank), which has an analogous folding pattern to the *R. sphaeroides* cytochrome c_2 (Meyer & Kamen, 1982) used in these experiments. The positions of lysine residues 95, 97, 99, 103, and 105 are indicated in the figure. The numbering is taken from the *R. sphaeroides* sequence, with the phenylalanine-102 and heme methionine and histidine ligands as references. This orientation places this lysine-rich protein segment and the exposed heme edge in closest approach to the reaction center. (B) The cytochrome c–reaction center electron-transfer complex. The figure shows the protein backbone structure for tuna cytochrome c (Brookhaven National Laboratory Protein Data Bank), which shares a common folding pattern to the horse heart cytochrome c used in these experiments (Meyer & Kamen, 1982). The surface shown represents that used to bind to the reaction center. The positions of phenylalanine-82 and lysine residues 13, 72, 73, 86, and 87, which have been determined by chemical modification to form the binding domain (Capaldi et al., 1982; Koppenol & Margoliash, 1982; Meyer & Kamen, 1982), are indicated in the figure. The numbering is taken from the horse cytochrome sequence. (C) Cytochrome c bound to the surface of negatively charged vesicles. In this orientation, lysine residues 86, 87, and 88 are in closest approach to the membrane, as is the first helix, which lies parallel to the membrane surface and has lysine residues at positions 5, 7, 8, and 13.

R. sphaeroides reaction center.[1] The *R. sphaeroides* and *Rp. viridis* reaction centers differ in that the *R. sphaeroides* reaction center contains no cytochrome subunit and reacts with water-soluble c cytochromes, while the *Rp. viridis* reaction center has a cytochrome subunit containing four hemes permanently fixed to it (Dutton & Prince, 1978). Although the two cytochromes are clearly unrelated, these data suggest that both position the heme in similar orientation with respect to the bacteriochlorophyll dimer.

By defining the optical x and y directions as described above, the dichroism for the cyt c–reaction center complex (Table III) yields the orientation for cytochrome c shown in Figure 12B. The heme is oriented 7.5° less perpendicular to the membrane and rotated by 32° about the heme normal compared to the cyt c_2–reaction center complex. The protein segment with residues 82–86, the end of the first helix (residues 13 and 14), and the end of the third helix (residues 71 and 72) lie closest to the reaction center binding site. Lysines-13, -72, -86, and -87 are all in position to form contacts with the reaction center. These residues are labeled in Figure 12B and define the binding site for cytochrome oxidase and cytochrome c reductase (Capaldi et al., 1982; Koppenol & Margoliash, 1982, Meyer & Kamen, 1982). The dichroism data suggest that the same site on the cytochrome c surface is used to bind to the reaction center. The position of phenylalanine-82 suggests that it may also make hydrophobic contacts with the reaction center.

Figure 12C shows how these assignments position cytochrome c in the complex with the negatively charge membrane. Residues 86, 87, and 88, which are all lysines, lie closest to the membrane. The next closest is the first helix, which is parallel to the membrane surface and has lysines at positions 5, 7, 8, and 13. Lysines-72 and -73 are also positioned closely enough to interact with the negatively charge surface. The phenylalanine-82 ring is directly over the heme. This orientation does not position the cytochrome c dipole moment (Koppenol et al., 1978; Koppenol & Margoliash, 1982) perpendicular to the membrane surface.

The dichroism data demonstrate that the interaction sites on cytochrome c and c_2 for the reaction center are different. This suggests that although the tertiary structures for the two cytochromes have been conserved, interaction domains on their surfaces have not been. Although the assignment of the optical x and y transitions to different heme directions would lead to different predictions for the cytochrome orientations, the dichroism data are consistant with the idea that the same site on the cytochrome c surface that is used to bind to cytochrome c oxidase and reductase is also used to bind to the reaction center. A different site, more directly facing the exposed heme edge, is indicated for cytochrome c_2.

The proposed binding domain on cytochrome c does not position the exposed heme cleft nearest to the membrane as in the case of cytochrome c_2. Unlike cytochrome c_2, the tilt of the closest approach to the exposed heme edge away from the reaction site suggests that rotation may be needed to assist rapid electron transfer to the reaction center. This is consistent with experiments that show electron transfer to the reaction center to be slowed by viscosity and cross-linking for cytochrome c, but not for cytochrome c_2 (Rosen et al., 1983). In order to maximize electron-transfer rates with cytochrome c oxidase and reductase, this would suggest that binding or reaction domains on these enzymes must be inclined to the membrane.

The ability to distinguish between the binding of cytochrome c and c_2 to the reaction center shows that this dichroism ap-

[1] Note that the in the article by Vermeglio et al. (1980) the oriented membranes are rotated by 90° compared to the definitions used here (Figure 1), so that their A_V and A_H correspond to our A_H and A_V, respectively.

proach can be used to examine how specific amino acid modifications affect cytochrome orientation and electron transfer in complexes with the reaction center. This approach can also be extended to study cytochrome *c* binding to the cytochrome *c* oxidase and reductase, and to examine the complexes formed between plastocyanin and photosystem I.

ACKNOWLEDGMENTS

This work was begun while I was in the laboratory of Dr. Jacques Breton, Service de Biophysique, CEN de Saclay, 91191 Gif-sur-Yvette, France. I gratefully acknowledge his enthusiastic support, instruction, and stimulating discussions. I am also indebted to Dr. Jau Tang (Argonne National Laboratory) for his instruction on nonlinear least-squares fitting procedures and to Dr. Chong-Hwan Chang (Argonne National Laboratory) for his help with the Evans and Sutherland display of the cytochrome *c* and c_2 structures.

Registry No. Cyt *c*, 9007-43-6; cyt c_2, 9035-43-2.

REFERENCES

Abdourakhmanov, I. A., Ganago, A. O., Erokin, K. E., Solov'ev, A. A., & Chugunov, V. A. (1979) *Biochim. Biophys. Acta 546*, 183–186.

Adar, F. (1978) in *The Porphyrins* (Dolphin, D., Ed.) Vol. III, pp 167–209, Academic, New York.

Bartsch, R. (1978) in *The Photosynthetic Bacteria* (Clayton, R. K., & Sistrom, W. R., Eds.) pp 249–279, Plenum, New York.

Breton, J., & Vermeglio, A. (1982) in *Photosynthesis* (Govindjee, Ed.) Vol. 1, pp 153–193, Academic, New York.

Capaldi, R. A., Darley-Usmar, V., Fuller, S., & Millet, F. (1982) *FEBS Lett. 138*, 1–7.

Chang, C.-H., Tiede, D. M., Tang, J., Smith, U., Norris, J., & Schiffer, M. (1986) *FEBS Lett. 205*, 82–86.

Cherry, R. J., Hsu, K., & Chapman, J. D. (1972) *Biochim. Biophys. Acta 267*, 512–522.

Crofts, A. R., & Wraight, C. A. (1983) *Biochim. Biophys. Acta 726*, 149–185.

Das, M., Haak, E. D., & Crane, F. L. (1965) *Biochemistry 4*, 859–865.

Deisenhofer, J., Epp, O., Miki, K., Huber, R., & Michel, H. (1984) *J. Mol. Biol. 180*, 385–398.

Deisenhofer, J., Epp, O., Miki, K., Huber, R., & Michel, H. (1985) *Nature (London) 318*, 618–624.

Dutton, P. L., & Prince, R. C. (1978) in *The Photosynthetic Bacteria* (Clayton, R. K., & Sistrom, W. R., Eds.) pp 525–570, Plenum, New York.

Dutton, P. L., Petty, K. M., & Prince, R. C. (1976) *Fed. Proc., Fed. Am. Soc. Exp. Biol. 35*, 1597.

Eaton, W. A., & Hochstrasser, R. M. (1967) *J. Chem. Phys. 46*, 2533–2539.

Fromherz, P. (1970) *FEBS Lett. 11*, 205–208.

Gouterman, M. (1978) in *The Porphyrins* (Dolphin, D., Ed.) Vol. III, pp 1–165, Academic, New York.

Haworth, P., Arntzen, C. J., Tapie, P., & Breton, J. (1982) *Biochim. Biophys. Acta 679*, 428–435.

Hoff, A. (1982) *Mol. Biol. Biochem. Biophys. 35*, 80–326.

Hofrichter, J., & Eaton, W. A. (1976) *Annu. Rev. Biophys. Bioeng. 5*, 511–560.

Hotani, H. (1984) *J. Mol. Biol. 178*, 113–120.

Johansson, L. B.-A., & Lindblom, G. (1980) *Q. Rev. Biophys. 13*, 63–118.

Ke, B., Chaney, T. H., & Reed, D. W. (1970) *Biochim. Biophys. Acta 216*, 373–383.

Koppenol, W. H., & Margoliash, E. (1982) *J. Biol. Chem. 257*, 4426–4437.

Kramer, H. J. M., Van Grondelle, R., Hunter, N. C., Westerhuis, W. H. J., & Amesz, J. (1984) *Biochim. Biophys. Acta 765*, 156–165.

Lubitz, W., Lendzian, F., Shceer, H., Gottstein, J., Plato, M., & Mobius, K. (1984) *Proc. Natl. Acad. Sci. U.S.A. 81*, 1401–1405.

Mar, T., & Gingras, G. (1984) *Biochim. Biophys. Acta 764*, 283–294.

Matthew, J. B., Weber, P. C., Salemme, F. R., & Richards, F. M. (1983) *Nature (London) 301*, 169–171.

Meyer, T. E., & Kamen, M. D. (1982) *Adv. Protein Chem. 35*, 105–212.

Meyer, T. E., Przysiecki, C. T., Watkins, J. A., Bhattacharyya, A., Simondsen, R. P., Cusanovich, M. A., & Tollin, G. (1983) *Proc. Natl. Acad. Sci. U.S.A. 80*, 6740–6744.

Moser, C. C., & Dutton, P. L. (1986) *Biophys. J. 49*, 23a.

Nabedryk, E., & Breton, J. (1981) *Biochim. Biophys. Acta 635*, 515–524.

Norris, J. R., Scheer, H., Druyan, M. E., & Katz, J. J. (1974) *Proc. Natl. Acad. Sci. U.S.A. 71*, 4897–4900.

Okamura, M. Y., Nelson, N., & Feher, G. (1982) in *Photosynthesis: Energy Conservation by Plants and Bacteria* (Govindjee, Ed.) Vol. 1, pp 195–272, Academic, New York.

Overfield, R. E., & Wraight, C. A. (1980a) *Biochemistry 19*, 3322–3327.

Overfield, R. E., & Wraight, C. A. (1980b) *Biochemistry 19*, 3328–3334.

Overfield, R. E., Wraight, C. A., & Devault, D. (1979) *FEBS Lett. 105*, 137–142.

Poulos, T. L., & Kraut, J. (1980) *J. Biol. Chem. 255*, 1022–1033.

Prince, R. C., Cogdell, R. J., & Crofts, A. R. (1974) *Biochim. Biophys. Acta 347*, 1–13.

Prince, R. C., Baccarini-Melandri, A., Hauska, G. A., Melandri, B. A., & Crofts, A. R. (1975) *Biochim. Biophys. Acta 387*, 53–56.

Rafferty, C. N., & Clayton, R. K. (1979) *Biochim. Biophys. Acta 546*, 189–206.

Rieder, R., Wiemken, V., Bachofen, R., & Bosshard, H. R. (1985) *Biochem. Biophys. Res. Commun. 128*, 120–126.

Rosen, D., Okamura, M. Y., & Feher, G. (1979) *Biophys. J. 25*, 204a.

Rosen, D., Okamura, M. Y., & Feher, G. (1980) *Biochemistry 19*, 5687–5692.

Rosen, D., Okamura, M. Y., Abresch, E. C., Valkirs, G. E., & Feher, G. (1983) *Biochemistry 22*, 335–341.

Salemme, F. R. (1976) *J. Mol. Biol. 102*, 563–568.

Snozzi, M., & Crofts, A. R. (1985) *Biochim. Biophys. Acta 809*, 260–270.

Steinemann, A., & Lauger, P. (1971) *J. Membr. Biol. 4*, 74–86.

Straley, S. C., Parson, W. W., Mauzerall, D. C., & Clayton, R. K. (1973) *Biochim. Biophys. Acta 305*, 597–609.

Takano, T., & Dickerson, R. E. (1981) *J. Mol. Biol. 153*, 79–115.

Tapie, P., Haworth, P., Hervo, G., & Breton, J. (1982) *Biochim. Biophys. Acta 682*, 339–344.

Teissie, J. (1981) *Biochemistry 20*, 1554–1560.

Tiede, D. M., & Dutton, P. L. (1981) *Biochim. Biophys. Acta 637*, 278–290.
Tiede, D. M., Choquet, Y., & Breton, J. (1984) in *Advances in Photosynthesis Research* (Sybesma, C., Ed.) Vol. 1, pp 669–672, Nijhoff/Junk, The Hague.
Vermeglio, A., & Clayton, R. K. (1976) *Biochim. Biophys. Acta 449*, 500–515.
Vermeglio, A., Breton, J., Barouch, Y., & Clayton, R. K. (1980) *Biochim. Biophys. Acta 593*, 299–311.
Wraight, C. A. (1979) *Biochim. Biophys. Acta 548*, 309–327.

Interaction between the Oligomycin Sensitivity Conferring Protein and the F_o Sector of the Mitochondrial Adenosinetriphosphatase Complex: Cooperative Effect of the F_1 Sector†

Alain Dupuis* and Pierre V. Vignais
Laboratoire de Biochimie, Département de Recherche Fondamentale, Centre d'Etudes Nucléaires de Grenoble, 85X, 38041 Grenoble Cedex, France

Received May 5, 1986; Revised Manuscript Received September 17, 1986

ABSTRACT: Beef heart mitochondrial oligomycin sensitivity conferring protein (OSCP) labeled with [^{14}C]-*N*-ethylmaleimide ([^{14}C]OSCP) at the only cysteine residue, Cys-118, present in the sequence [Ovchinnikov, Y. A., Modyanov, N. N., Grinkevich, V. A., Aldanova, N. A., Trubetskaya, O. E., Nazimov, I. V., Hundal, T., & Ernster, L. (1984) *FEBS Lett. 166*, 19–22] exhibits full biological activity in a reconstituted F_o–F_1 system [Dupuis, A., Issartel, J. P., Lunardi, J., Satre, M., & Vignais, P. V. (1985) *Biochemistry 24*, 728–733]. The binding parameters of [^{14}C]OSCP with respect to the F_o sector of submitochondrial particles largely depleted of F_1 and OSCP (AUA particles) have been explored. In the absence of added F_1, a limited number of high-affinity OSCP binding sites were detected in the AUA particles (20–40 pmol/mg of particles); under these conditions, the low-affinity binding sites for OSCP were essentially not saturable. Addition of F_1 to the particles promoted high-affinity binding for OSCP, with an apparent K_d of 5 nM, a value 16 times lower than the K_d relative to the binding of OSCP to F_1 in the absence of particles. Saturation of the F_1 and OSCP binding sites of AUA particles was attained with about 200 pmol of both F_1 and OSCP added per milligram of particles. The oligomycin-dependent inhibition of F_1-ATPase bound to AUA particles was assayed as a function of bound OSCP. At subsaturating concentrations of F_1, the dose–effect curves were rectilinear until inhibition of ATPase activity by oligomycin was virtually complete, and maximal inhibition was obtained for an OSCP to F_1 ratio of 1 (mol/mol). Experiments carried out with F_1 labeled in the β subunit by [^{14}C]dicyclohexylcarbodiimide ([^{14}C]F_1) indicated that [^{14}C]F_1, in spite of extensive inactivation [Pougeois, R., Satre, M., & Vignais, P. V. (1979) *Biochemistry 18*, 1408–1413], was able to bind to the AUA particles specifically, even in the absence of OSCP, as does native F_1, with a K_d value of 60 nM. OSCP enhanced by about 6 times the binding affinity of [^{14}C]F_1 for the AUA particles but not its binding capacity. The mutual promotion of OSCP and F_1 for binding to AUA particles was corroborated by a double-labeling experiment carried out with [^{3}H]OSCP and [^{14}C]F_1. Whereas the binary associations between OSCP and particles or between F_1 and particles were readily reversible, the ternary complex formed by particles, F_1, and OSCP was much more difficult to dissociate. These results make it likely that OSCP is a key component required for the stability of the mitochondrial F_1–F_o complex. Photoirradiation with an azido derivative of OSCP in the presence of AUA particles resulted in the photolabeling of mainly the β subunit of F_1, whereas, in the absence of particles, azido-OSCP reacted with both the α and β subunits of F_1, with strong preference for the α subunit, suggesting that F_1 undergoes conformational changes when it binds to the F_o sector of the ATPase complex.

The coupling between the catalytic sector F_1[1] and the proton channel F_o of the mitochondrial ATPase complex is central to the mechanism of ATP synthesis. The oligomycin sensitivity conferring protein (OSCP) (Mc Lennan & Tzagoloff, 1968) is thought to be one of the peptides that link the catalytic sector F_1 of the mitochondrial ATPase complex to the membrane sector F_o (Mc Lennan & Asai, 1968). F_1 per se is insensitive to oligomycin; however, in the reconstituted F_1–F_o complex, F_1 becomes sensitive to oligomycin, a ligand of F_o, provided that OSCP is added to the F_1–F_o complex [see Tyler (1984) for review]. Although OSCP is recognized as a key factor in oxidative phosphorylation, its exact function remains enigmatic, partly due to the lack of a precise assessment of the

† This work was supported by grants from the Centre National de la Recherche Scientifique (CNRS/UA 1130), the Institut National de la Santé de la Recherche Médicale, and Université Scientifique Technologique et Médicale de Grenoble, Faculté de Médecine.

[1] Abbreviations: OSCP, oligomycin sensitivity conferring protein; [^{14}C]OSCP, OSCP labeled by [^{14}C]NEM; TPCK-trypsin, trypsin treated by L-1-(tosylamido)-2-phenylethyl chloromethyl ketone; ATPase, adenosinetriphosphatase; F_1, catalytic sector of H^+-dependent ATPase; F_o, membrane sector of H^+-dependent ATPase; [^{14}C]F_1, F_1 labeled in the β subunit by [^{14}C]DCCD; $NaDodSO_4$, sodium dodecyl sulfate; NEM, *N*-ethylmaleimide; DCCD, dicyclohexylcarbodiimide; AP-OSCP, azidophenacyl-OSCP; AUA particles, submitochondrial particles depleted of F_1 and OSCP after treatment with urea and ammonia; IgG, immunoglobulin G; Tris, tris(hydroxymethyl)aminomethane; MES, 4-morpholineethanesulfonic acid; EDTA, ethylenediaminetetraacetic acid.

0006-2960/87/0426-0410$01.50/0